

## ASA-LSTM-based brain tumor segmentation and classification in MRI images

Dhyanendra Jain<sup>1\*</sup>, Amit Kumar Pandey<sup>2</sup>, Alok Singh Chauhan<sup>3</sup>, Jitendra Singh Kushwah<sup>4</sup>, Neeta Saxena<sup>5</sup>, Rajeev Sharma<sup>6</sup> and Venkata Durga Prasad Sambrow<sup>7</sup>

Associate professor, Department of CSE-AIML, ABES Engineering College, Ghaziabad Affiliated to AKTU, U.P, India<sup>1</sup>

Associate professor, Department of CSE-DS, ABES Engineering College, Ghaziabad Affiliated to AKTU, U.P, India<sup>2</sup>

Associate Professor, School of Computer Applications and Technology, Galgotias University, Greater Noida, India<sup>3</sup>

Associate Professor, Department of Information Technology, Institute of Technology and Management, Gwalior, India<sup>4</sup>

Associate Professor, Department of Engineering Mathematics, LaxmiNarain College of Technology Excellence, Bhopal, India<sup>5</sup>

Assistant Professor, Department of Computer Science, Government College Kailaras, Morena, India<sup>6</sup>

Assistant Professor, Department of Computer Science & Engineering - Data Science, Chalapathi Institute of Engineering & Technology, Guntur, India<sup>7</sup>

Received: 17-August-2023; Revised: 22-May-2024; Accepted: 24-May-2024

©2024 Dhyanendra Jain et al. This is an open access article distributed under the Creative Commons Attribution (CC BY) License, which permits unrestricted use, distribution, and reproduction in any medium, provided the original work is properly cited.

### Abstract

Brain tumors form when groups of abnormal cells develop in the brain and have the capacity to infiltrate nearby tissues. Early detection of brain tumors is essential for treating cancer patients and maximizing their survival rates. The brain tumor segmentation (BraTS – 2020) dataset is utilized in this research for segmentation and classification. Min-max normalization and median filter are used in this experiment for data pre-processing after which, the pre-processed data is then fed to DenseNet-201 for extracting features from magnetic resonance images (MRI). Next, a whale optimization algorithm (WOA) is used for effective selection of features. This work proposes an attentive symmetric auto-encoder (ASA)-based segmentation that returns similar code for two variants, and a long short-term memory (LSTM) method for effective classification. The performance of the proposed ASA-LSTM method is estimated by utilizing various tumor regions known as tumor core (TC), enhancing tumor (ET) and whole tumor (WT). The proposed method achieves accuracies of 99.48%, 99.44%, and 99.32% for TC, ET, and WT tumor regions, respectively. These results compared with other existing methods, including convolutional neural network (CNN), artificial neural network (ANN), and recurrent neural network (RNN). The proposed method is found to be effectively than other existing techniques in the segmentation and classification of brain MRI images.

### Keywords

Attentive symmetric auto-encoder, Brain tumor, Long short-term memory, Median filter, Min-max normalization and Whale optimization algorithm.

## 1.Introduction

The human brain is an important organ in the nervous system of humans which is responsible for the appropriate functioning of many basic vital activities of an individual's life [1–4]. The brain gathers signals from the organs of the body, handles processing, and manages the decisions and resultant actions [5-7]. A brain tumor is a collection of unmanaged cancer cells which grow around the brain [8].

Brain tumors are divided into two types namely, primary tumors that grow in the spinal cord or brain alone, and secondary tumors that are also known as brain metastases which grow anywhere in the human body and spread to the brain [9–12]. There are various types of scan imaging systems such as computed tomography (CT), electroencephalogram (EEG) and magnetic resonance images (MRI), which are used to provide significant information about the vicinity, dimension, and metabolism of the tumor in the cerebrum [13–16]. These systems are combined to produce the major information about cerebrum tumors

\* Author for correspondence

[5]. MRI is a non-intrusive system that utilizes the signals of radio recurrence to develop interior images under the influence of an extremely attractive field [17–20]. The MRI system gives different types of contrast images of the tissue, and eventually produces significant auxiliary information along with the analysis of tumor segmentation through its sub-regions [21, 22].

The detection of brain tumors using MRI images is a difficult task due to the requirements [23–25]. The accuracy of brain tumor diagnosis is amplified by the process of segmentation [26]. In recent times, methods depending on deep learning (DL) have majorly been utilized in medical image for segmentation [27]. There is a chance for acquiring many noises like salt and pepper, speckle and Gaussian while obtaining the MRI images [28]. So, the technique of noise removal is important for decreasing the noise. The selection of features plays a major role in the classification part because it decreases the evaluation time and maximizes the performance of classification [29]. The application of DL produces an ideal solution because it extracts many prominent features from the entire image than the manually extracted features [30]. The most recently adopted techniques for segmentation depend on DL that needs a masked image for an expected outcome [31]. These labels support or guide the learning process in the segmentation stage, but this process takes more time for computing [32]. To overcome these issues, the process of segmentation based on attentive symmetric auto-encoder (ASA) is utilized, that returns similar code for two variants with symmetrical positions.

The major aims of the paper are described below:

- ASA method is proposed to segment the brain tumors using MRI images.
- Transformers encode the coordinates for an image patch to evaluate correlations between various positions. The proposed ASA is a symmetrical approach with a new position encoding technique that returns similar code to two variants, but at symmetrical locations. Transformers that involve encoding, improve vision features by highlighting correlations among the areas of the contralateral brain.
- The performance of the segmentation process is evaluated by using dice score coefficient (DSC) and hausdorff distance (HD) measures, whereas the classification method is estimated by utilizing accuracy, precision, and F1-Score on various tumor regions that are, tumor core (TC), enhancing tumor (ET) and whole tumor (WT).

This rest of the research paper is designed as follows: the related existent researches in brain tumor segmentation (BraTS) and classification is given in section 2. The proposed method is explained in section 3. The outcomes and comparative analysis of this research are discussed in section 4, while conclusion of this research is given in section 5.

## 2.Literature survey

Walsh et al. [33] implemented a lightweight U-Net method to segment brain tumor using MRI images. U-Net is a fully connected convolutional neural network (CNN) used for an effective segmentation of images. U-Net deep neural network (DNN) fits in different tasks of broad ranging applications, and is specifically useful when the input is in image format. The implemented method generated real-time segmentation of MRI scans and did not require huge data for training. But this method was not suitable for detecting a tumor in its early stages.

Kibriya et al. [34] introduced a novel CNN architecture for multiple-class classification of brain tumors using MRI images. The introduced CNN architecture classified three kinds of brain tumors: glioma, pituitary and meningioma. Huge experiments were performed to conclude the layers of CNN and hyperparameters before reaching the last result. The introduced method decreased the layer count and learnable parameters for classification. However, the low-grade and high-grade tumors were not classified by this method.

Mowlani et al. [35] presented two training algorithms for segmentation and classification of MRI brain tumors. After features were extracted, images were classified using two ML techniques, (i) support vector machine (SVM), that depended on features selected by grasshopper optimization algorithm – SVM (GOA-SVM), and (ii) DNN optimized with genetic algorithm deep neural network (GA-DNN). These methods classified brain tumors as benign and malignant. GOA algorithm was employed for adjusting a classification parameter in SVM, to maximize the effectiveness and reduce the issue of overfitting. The whole image dataset was used for classification, which resulted in negligence while extracting objects of interest, which was a major drawback of this work.

Amin et al. [36] suggested a secured two-qubit quantum method for segmentation and classification of MRI brain tumors. The suggested technique contained three stages. At the initial stage, the MRI data of the patient was encrypted and decrypted by

secure hash algorithm (SHA)-256 algorithm for security of brain data. The decrypted images were given to a 2-qubit quantum method named Javeria (J). The Quantum method used for classification had three layers, double dense and single keras with softmax. The images were classified and given as input to a segmentation method. Further, segment convolutional neural network (SegCNN) was deployed for segmentation. The suggested method has 11 layers which were trained on the chosen batch size and Adam optimizer. The method analyzed the features of super-voxel to minimize the process of computation. The method was not applicable for real time data fusion and cascading.

Deepa et al. [37] developed the chronological jaya honey badger algorithm (CJHBA) for segmentation and classification of MRI brain tumors. The developed CJHBA was a combination of chronological, Jaya, and honey badger algorithms (HBA). The features were extracted by the CNN for better classification. Further, classification was done by taking the extracted features and giving them as input to the deep residual network (DRN), where training was done by utilizing the developed CJHBA. The introduced method gave higher accuracy with lesser time execution. Yet, the method did not identify the substructure of tumor regions.

Rao and Karunakara [38] implemented a Kernal support vector machine-social ski driver (KSVM-SSD) for the detection and classification of MRI brain tumors. The extraction of features was done by the fusion of gray level co-occurrence matrix (GLCM) and spatial GLCM (SGLCM) methods. The selection of features was done by employing Harris hawks optimization (HHO). Then, brain tumors were classified as benign and malignant by KSVM, while the malignant tumor were classified as small, medium, or large by the social ski driver (SSD) optimization algorithm. The implementation had lesser computation complexity and by using an optimization algorithm, it attained features of high relevancy and less redundancy.

Nanda et al. [39] suggested a classification method that included hybrid salience k-mean segmentation method through usage of social spider optimization (SSO) algorithm in radial basis neural network (RBNN). The segmentation technique of hybrid saliency map along with k-means cluster was utilized for segmenting tumor regions. The feature extraction was implemented through multiple resolution wavelet transform, principal component, kurtosis, skewness

and cosine transform. Then, classification was performed by RBNN through optimized cluster centre by SSO. The RBNN along with gaussian kernel reduced complexity in the classification.

Ilhan et al. [40] implemented a tumor localization and enhancement model with U-net for segmentation of MRI brain tumors. At the initial stage, histogram-based nonparametric tumor localization method, was taken to localize the tumorous regions, whereas the implemented tumor enhancement model was utilized for improving localized regions, to maximize the visual appearance of low-contrast or indistinct tumors. The outcome images were given to U-net architecture for segmentation. The implementation had lesser computation complexity. The method was not applicable for real time data fusion and cascading.

Habib et al. [41] executed segmentation of brain tumor in MRI images by introducing threshold segmentation and watershed algorithm, next the brain tumors were classified by various classifiers from extracted features. The introduced method included image acquisition, pre-processing of image, segmentation and feature extraction. Various classifiers were utilized for classifying brain tumors from dataset. Yet, the method did not identify the substructure of tumor regions.

Khairandish et al. [42] suggested hybrid CNN-SVM for BraTS and classification. The CNN along with numerous techniques that were not handcrafted, were used to extract the features. The presented method integrated CNN and SVM for classification and threshold-based segmentation.

Budati and Katta [43] suggested a machine learning technique (MLT) for recognizing and classifying tumor in MRI images. The chan-veese (C-V) method was deployed for segmenting tumors by choosing accurate initial point. Next, tumor features were extracted through GLCM and significant features were selected. At last, a two-class classifier was introduced through SVM and the performance was analyzed by k-nearest neighbor (KNN).

Nawaz et al. [44] developed a hybrid-brain-tumor-classification (HBTC) for segmentation and classification. The developed method enhanced the diagnosis performance. The brain MRI dataset was given as input to HBTC technique, then the pre-processing, and segmentation was used for localizing tumor area. From segmented data, the co-occurrence

matrix (COM), the run-length matrix (RLM) and gradient features were extracted.

Chahal and Pandey [45] introduced a hybrid weighted fuzzy k-means (WFKM) method for segmentation and classification. The introduced method was dependent on weights fuzzification that was processed in spatial context with the illumination technique which tackled the problem of multimembers pixel and also exponentially maximized the count of iterations. The segmented image was next used for the identification of tumor kinds as malignant and benign.

Rahman and Islam [46] presented a parallel deep convolutional neural network (PDCNN) method for extracting both local and global features, and to deal with overfitting issue through dropout regularization. Initially, input images were resized, and then grayscale transformation was experimented on them, to minimize the complexity. Next, data augmentation was employed for increasing count of datasets. The advantages of parallel pathways were acquired through integration of two DCNNs with various window sizes, which allowed the method to learn global and local data.

Tseng and Tang [47] implemented an optimized eXtreme gradient boosting (XGBoost) method for image processing and feature selection, to identify brain tumors. The images were enhanced through contrast-limited adaptive histogram equalization (CLAHE) technique. Additionally, K-means method divided images into sections where segmentation assisted the particular area of interest. Particle swarm optimization (PSO) was employed for selecting characteristics.

Gupta and Bibhu [48] developed an improved invasive bat (IIB)-based DRN method by integrating enhanced invasive weed optimization (IWO) and bat algorithm (BA). Tumor segmentation of MRI images had high

impact on detecting brain tumor at the initial phase. The DL-based technique produced effective detection outcomes with MRI images. The features were obtained from tumor areas which were utilized for enabling effective detection procedure with DRN.

Saurav et al. [49] introduced a lightweight attention-guided CNN (AG-CNN) technique for BraTS and classification. The introduced method utilized channel attention blocks for concentrating on the related areas in the image to classify the tumor. This method utilized skip connection through global average pooling for integrating features from various phases. The introduced method helped to extract significant features from MRI images of variant tumors as well as normal brain. From the overall analysis, it is evident that the existing methods have drawbacks like, not being suitable for detecting a tumor in the early stages, low-grade and high-grade tumors were not classified, neglecting the objects of interest to be extracted, not being applicable for real time data fusion and cascading, and not identifying the substructure of tumor regions.

### 3. Materials and methods

In the proposed methodology, the ASA and long short-term memory (LSTM) are proposed for effective segmentation and classification of brain tumors. The imaging dataset of BraTS – 2020 is employed in the proposed method. The Min-Max normalization and median filter are utilized in the pre-processing stage while the DenseNet-201 is utilized for the extraction of features from MRI images. The whale optimization algorithm (WOA) algorithm is deployed to select the features. The proposed ASA method is utilized for the image segmentation process, and LSTM is utilized for the effective classification. The pictorial representation of the proposed methodology is represented as *Figure 1*.

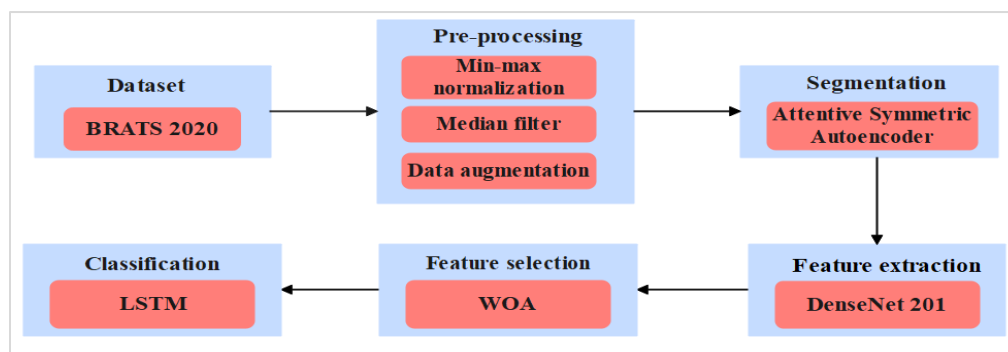


**Figure 1** Overall process of BraTS and classification

### 3.1 Dataset

The dataset utilized for the research is BraTS 2020 [50] taken from Kaggle which contains the records of 369 patients. The total number of tumorous and non-tumorous 2-dimensional fluid-attenuated inversion recovery (2D-FLAIR) axial images of patients is 57,195 images. Every image in the dataset has four modalities: T1, T1c, T2 and FLAIR. The images used for training are 369, while 169 are used for testing, and 125 are used for validation. *Figure 2* describes the sample images of the dataset.

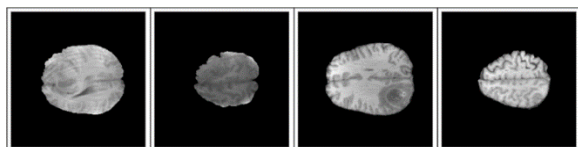


**Figure 2** Sample images of dataset

### 3.2 Pre-processing

Data pre-processing is a process of converting raw data into a suitable format, because datasets from various resources contain incomplete data. For further analysis, the data needs to be normalized, filtered, and augmented.

#### 3.2.1 Min-Max normalization

Normalization of data is a process of preprocessing the input data. The min-max normalization of images is done before being fed into the segmentation phase and is represented in Equation 1.

$$f(x, y) = \frac{f(x, y) - Z_{min}}{Z_{max} - Z_{min}} \quad (1)$$

Where  $f$  represents the brain image,  $x$  and  $y$  represent pixel positions in the image,  $Z_{min}$  and  $Z_{max}$  represent the minimum and maximum pixel values respectively. The normalization of intensity scales the values of intensity between  $[0, 1]$ , as well as resizes the images to  $227 \times 227$  before feeding them into segmentation.

#### 3.2.2 Median filter

Median filter is a process that uses nonlinear mechanism to eliminate noise from MRI brain tumor images. The removal of salt and pepper noise is specifically effectual [51]. It works through shifting pixels in an image, and adjusting each score along a median score of an adjacent pixel. A pixel is identified by distributing all of its values in a neighborhood pattern into a mathematical order and is then changed to consider mean pixel score. The median filter eliminates noise efficiently without reducing image sharpness and is given in Equation 2.

$$f(x, y) = \text{median}\{g(s, t)\} \quad (2)$$

where  $(s, t) \in S_{xy}$

Where  $S_{xy}$  describes the set of categories in a rectangular sub-MR image window which has its center at  $(x, y)$ . Further,  $f(x, y)$  describes a restored image and  $g(s, t)$  describes the measured and corrupted area under  $S_{xy}$ .

#### 3.2.3 Data augmentation

Data augmentation is a technique that artificially increases the size of dataset images by making small changes or modifications in the existing data. Various modifications are utilized to maximize the size of the dataset. By utilizing data augmentation, the chances of overfitting is reduced and the performance of the model is maximized. A range rotation, translation of height and weight, range of brightness, and vertical and horizontal flips are performed. To improve the performance of method, 20 parameters are employed for improving every image. Next, the data augmentation size of the dataset is increased. After preprocessing and augmentation, the brain images are given as input to the proposed ASA for segmenting the brain tumor images.

### 3.3 Image segmentation

BraTS is an analysis of medical images that separates brain tumors from normal brain tissue in MRI scans. MRI is the major imaging technique used to capture brain images.

#### 3.3.1 ASA

For image segmentation, an ASA is utilized, which is trained to acquire the weights of the model for adapting brain MRI image segmentation. The proposed ASA has encoder and decoder pairs along the symmetric position encoding (SPE) and loss of attentive reconstruction. In the process of self-supervised training of ASA, the input of 3D images are separated into non-overlapping images of size  $s \times s \times s$ .  $P\%$  of the image patches are masked at random and only the unmasked patches are shown. The parameters used in ASA are learning rate 0.001, epochs 100, activation function hyperbolic tangent and loss function mean squared error (MSE). After linear projection, every shown patch is fed to a feature vector that is updated with the SPE for generating the input for the encoder. The output of the encoder has similar vector counts as its input. In learnable vector mask, the tokens are similar vectors updated with various SPE methods. Every mask token is referred to the masked image patch. The outcome of the encoder is added along with mask tokens to produce input for the decoder. The decoder reforms whole image patches, and masked images alone are utilized for evaluating the developed loss.

**3.3.1.1 Attentive reconstruction loss**

The regions of flattened recovery are less and useful for improving the methods used to represent the harvest discriminates. Here, an Attentive Reconstruction Loss function which focuses on significant areas of brain MRI is proposed. To evaluate 3-dimensional (3D) data of the image patch, gradient-based measure for 3 images is implemented. Through 3dimensional voxel-based extension of the 2dimensional (2D) histogram of oriented gradients (3DVHOG) method, the measured gradient vector  $\vec{g} = (g_x, g_y, g_z)$  for every voxel is considered as filter mask. In spherical coordinates, measurable  $\theta$  and  $\phi$  scalars are utilized as given in Equation 3.

$$\theta = \cos^{-1} \left( \frac{g_z}{\sqrt{g_x^2 + g_y^2 + g_z^2}} \right), \tag{3}$$

$$\phi = |\text{atan2}(g_y, g_x)|$$

For every image patch, a 2D histogram  $G$  is developed, and the number of bins is  $b \times b$ . To evaluate  $G$  values, every image patch voxel is traversed.

Consider  $\theta, \phi$  represents the present voxel orientation. Initially, the voxel bin indexes are determined as  $r = [\theta/(\pi/b)]$ ,  $c = [\phi/(\pi/b)]$ , then the  $\|\vec{g}\|$  (present voxel gradient magnitude) is gathered to correlation bin  $(r, c)$  of 2D histogram  $G$ . After computing whole image patch voxels,  $L_2$  norm is processed on  $G$  which is the patch histogram. The average of  $G$  as  $\bar{G}$  for every image patch is measured.  $G$  is normalized between whole  $N$  masked image areas to categorize related significance  $P_i$  as done in Equation 4.

$$P_i = \frac{\bar{G}_i}{\sum_{i=1}^N \bar{G}_i} \tag{4}$$

The loss function considers MSE for measuring the difference in pixel levels among the retrieved image regions and actual ones, after which closer attention is given to significant brain areas by gradient-based weight  $P_i$ . The whole loss is represented in Equation 5.

$$L(X, Y) = \sum_{i=1}^N \left( P_i \cdot \sum_j^M (X_{ij} - Y_{ij})^2 / M \right) \tag{5}$$

Where  $X, Y$  represents the reconstructed and actual images,  $N$  represents the count of masked image patches in the image,  $M$  represents a voxel number in the image patch, and  $X_{ij}$  and  $Y_{ij}$  represent the  $j - th$  voxel of  $i - th$  patches in images  $X$  and  $Y$ , respectively.

**3.3.1.2 Symmetric position encoding**

The brain structures are observed according to the symmetry of left-right in the utilization of SPE

method. This SPE minimizes the difference in encoding between two symmetric image locations and helps the method to take the best features from the two corresponding areas. The patches in same horizontal level, position the encoding of the top left, and are highly variant than top right, although those areas have same contents. By utilizing the proposed SPE, the leftmost and rightmost (similar row) share a similar encoding. Consider  $T \times H \times W$ ,  $(t, h, w)$  represents the image patch number and corresponds to the image patch. The mathematical formula of SPE is represented in Equations 6 and 7,

$$Pos = (T^2 \cdot t + H \cdot h - |W/2 - w| + W/2) / (1000^{2i/D}) \tag{6}$$

$$PE(t, h, w, 2i) = \sin(pos), PE(t, h, w, 2i + 1) = \cos(pos), \quad 1 \leq i \leq \lfloor D/2 \rfloor \tag{7}$$

Where  $D$  represents a SPE vector dimension number that is assigned to the image patch embedding channel number.

$PE(\cdot)$  gives  $2i - th / (2i + 1) - th$  component of SPE vector for  $(t, h, w)$  patch. The SPE technique is utilized two times, one for embeddings of patches and another, for mask tokens. The segmented brain MRI images are given as input to DenseNet-201 for extracting the features.

**3.4 Feature extraction**

Feature extraction means a process of converting original information to numerical features, which is performed while protecting data in the original dataset. After feature extraction, it provides better outcomes than applying the raw data to the method directly. DenseNet-201 is utilized for the extraction of features from brain MRI segmented images.

**3.4.1 DenseNet-201**

The DenseNet-201 is a transfer learning method of DL where the past issues are reutilized to resolve the existing issues [52]. The features of BraTS 2020 dataset are extracted by DenseNet-201 method on lower and upper dense blocks which contain four stages of dense blocks, that is differentiated by the number of layers in every block. Five features namely, contrast, correlation, variance, entropy and inverse difference moment (IDM) are extracted by DenseNet-201. The parameters used in DenseNet-201 are depth 201, size 77MB and 20.0 parameters. The textual features are extracted from segmented images that assure a huge success rate for further stages. The features utilized in this research are evaluated as under (Equation 8):

**(a) Contrast**

$$f_1 = \sum_{n=0}^{N_g-1} n^2 \sum_{i=1}^{N_g} \sum_{j=1}^{N_g} p(i, j) \quad (8)$$

Where,  $N_g$  represents many grey levels in the actual image.

**(b) Correlation**

The grey levels' linear dependency on neighboring pixels is denoted by the feature of correlation. The statistical relationship among two variables is represented by correlation which is represented as Equation 9,

$$f_2 = \frac{\sum_i \sum_j (i) p(i, j) - \mu_x \mu_y}{\sigma_x \sigma_y} \quad (9)$$

Where  $\mu_x, \mu_y, \sigma_x, \sigma_y$  are the mean and standard deviation of the input image in row and column-wise order.

**(c) Variance**

Variance is a calculation of values dispersion around the mean. Variance is also referred to as the calculation of how far values of gray are spread out in the input image, which is represented as Equation 10.

$$f_3 = \sum_i \sum_j (i - \mu)^2 p(i, j) \quad (10)$$

Where  $\mu$  represents the mean of all images.

**(d) Entropy**

The distribution of gray level randomness is denoted by entropy. Entropy is expected to be large when the gray levels are randomly distributed in the image, and is represented in Equation 11,

$$f_4 = \sum_i \sum_j p(i, j) \log(p(i, j)) \quad (11)$$

**IDM**

The image smoothness information is represented by IDM. IDM is expected to be large when pixel gray levels are the same, and it is calculated in Equation 12,

$$f_5 = \sum_i \sum_j \frac{1}{1+(i-j)^2} p(i, j) \quad (12)$$

The features are generally utilized for brain MRI classification and are given as input for feature selection and further classification.

**3.5 Feature selection**

WOA is utilized for feature selection of brain MRI images. WOA is a population-based algorithm which is simulated using bubble-net feeding of whales [53]. The parameters used in WOA are, search agent 40, 500 iterations and [0, 1] random number. Every solution is estimated according to the fitness functions, accuracy of solution acquired through KNN classifier and count of chosen features in solution. To search for prey, the

whales swim spirally in the shape of six to develop bubbles. The shark traps the prey on a surface and hunts it. WOA contains two phases, exploitation and exploration that represent the hunting process of whales. The exploitation stage denotes a spiral attack and the exploration stage denotes a random search for the prey.

**3.5.1 Exploitation stage**

The exploitation stage represents the process of six-shape attacking whales, as given in Equation 13. As “6” shape attacking depicts whales making two movements towards a prey to hunt it. The movements decrease the path of encircling and spiral-shaped.

To represent a movement of encircling, Equations 13 and Equation 14 are utilized, wherein (Equation 14) represents the best-find solution and describes the solutions to update its positions.

$$\vec{D} = |\vec{C} \cdot \vec{X}^* - \vec{X}(t)| \quad (13)$$

$$\vec{X}(t + 1) = X^*(t) - \vec{A} \cdot \vec{D} \quad (14)$$

Where,  $X^*$  represents best-find solution,  $t$  represents the present iteration of the algorithm,  $A$  and  $C$  represent coefficient vectors and are numerically measured in Equations 15 and 16.

$$\vec{A} = 2\vec{a} \cdot \vec{r} - \vec{a} \quad (15)$$

$$\vec{C} = 2 \cdot \vec{r} \quad (16)$$

In Equations 15 and 16,  $a$  and  $r$  represent two parameters for measuring the above-mentioned vectors.  $r$  represents a parameter value in range of [0,1], and  $a$  represents the variable linearly decreasing from 2 to 0. The movement of a shrinking encircle is calculated by Equation 17,

$$a = a - t \frac{2}{max\_iteration} \quad (17)$$

Where  $max\_iteration$  denotes the maximum iterations. The distance among the present solution and good solution outcomes is in a spiral-shaped path. Equation 18 denotes the process of measuring the movement of a spiral.

$$\vec{X}(t + 1) = D' e^{lb} \cos(2\pi l) + \vec{X}^*(t) \quad (18)$$

Where  $D'$  denotes distance between whale and prey,  $b$  denotes a shape of a spiral, and  $l$  denotes a random number in the range of [-1, 1]. As described before, the whale utilizes two movements in the hunting process. So, the two movements need to be utilized in the optimization process. Following this, WOA deploys the random number  $p$  to choose among them, as represented in Equation 19, which represents the

process of choosing among the two movements. The WOA takes a similar probability for both movements.  $X(t + 1)$

$$= \begin{cases} \vec{X}(t + 1) = X^*(t) - \vec{A} \cdot \vec{D} & \text{if } (p < 0.5) \\ \vec{X}(t + 1) = D' e^{lb} \cos(2\pi l) + \vec{X}^*(t) & \text{if } (p \geq 0.5) \end{cases} \quad (19)$$

**3.5.2 Exploration stage**

The exploration stage stretches the search space for identifying new prey. The preceding stage fully depends on the best-find solution, wherein this exploration stage tries to find new spaces. Equations 20 and 21 represent mathematical formulae of the exploration stage.

$$\vec{D} = |\vec{C} \cdot \vec{X}_{rand} - \vec{X}| \quad (20)$$

$$\vec{X}(t + 1) = \vec{X}_{rand} - \vec{A} \cdot \vec{D} \quad (21)$$

Where  $\vec{X}_{rand}$  represents a whale chosen from the present population, and  $\vec{A}$  represents random values vector.

For moving away from the best-find solution, random values vector  $\vec{A}$  should be out of range  $[-1, 1]$ . The necessary features are selected by utilizing WOA and given as input to the LSTM classifier for classification of brain tumors.

**3.6 Classification**

For classification of brain tumors, the LSTM classifier is utilized. The selected feature images by WOA are given as input to LSTM for effective classification. The relevant features are selected by WOA, which reduces the dimensionality of the model and maximizes the classification accuracy. An LSTM block has three gate types known as input, output and forget gates, and the structure of gates is represented in Figure 3.

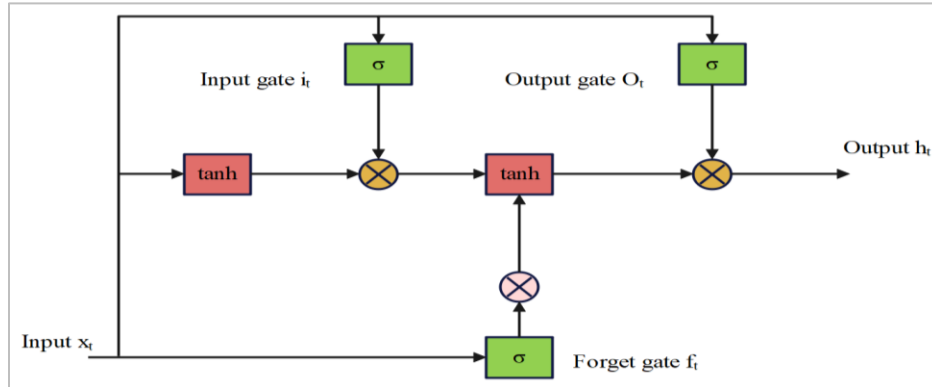


**Figure 3** Structure of input, output and forget gates

The parameters used in LSTM are learning rate = 0.005, batch = 64, dropout = 0.5 and hidden node number = 32. The number of new data updated to the cell state is represented in the input gate, while the data to be damaged from the cell is represented in the forget gate, and data required as output is represented in the output gate. These three gate structures are utilized in LSTM for data protection and control. LSTM cell structure majorly utilizes two functions known as tanh and sigmoid function. At last, it filters the cell state that goes with the activation function that in turn predicts which portion must appear as the output of a present LSTM unit at timestamp (t). Here, cell state is memory of LSTM, present moment is present time (t) and output of LSTM is the classified types of brain tumors. The mathematical representation of input, output and forget gate are given as Equations 22 to 24.

$$i_t = \sigma(\omega_i[h_{t-1}, x_t]) + b_i \quad (22)$$

$$o_t = \sigma(\omega_o[h_{t-1}, x_t]) + b_o \quad (23)$$

$$f_t = \sigma(\omega_f[h_{t-1}, x_t]) + b_f \quad (24)$$

Where  $i_t, o_t$  and  $f_t$  represent the input, output and forget gates,  $\sigma$  represents the sigmoid function,  $\omega_x$  represents the weight for the respective gate (x),  $h_{t-1}$  represents previous software transactional memory (STM) block output at timestamp  $t - 1$ ,  $x_t$  shows input at the present timestamp, and  $b_x$  shows the biases for the respective gate (x). The mathematical representation of cell state, candidate cell state and final output are numerically expressed in Equations 25 to 27.

$$\tilde{c}_t = \tanh(\omega_c[h_{t-1}, x_t] + b_c) \quad (25)$$

$$c_t = f_t * c_{t-1} + i_t \times \tilde{c}_t \quad (26)$$

$$h_t = o_t \times \tanh(c_t) \quad (27)$$

Where,  $c_t$  describes cell state at timestamp (t),  $\tilde{c}_t$  describes a candidate for cell state at timestamp (t), and  $h_t$  represents the output of the present LSTM block at timestamp (t). Output  $h_t$  at present LSTM block goes along the softmax layer to get output.



Measuring result of the input and output gate separately does not provide effective performance so, result from the input and output gate is differentiated by factor  $1 - f_t$ . This supports maximization of cell state for further layer in the input and output gate, as is described as Equation 28:

$$C_t = f_t \times C_{t-1} + (1 - f_t) \times \bar{C}_t \quad (28)$$

### 3.6.1 Softsign activation function

Softsign is a kind of activation function that is employed in LSTM. The features obtained using WOA are combined with the LSTM and then are given to the Softsign classifier in a fully connected manner to perform the classification of malware. Softsign activation function maps have a large probability value, and obtain a better classification performance. The Softsign is a quadratic polynomial which is represented using the Equation 29 as follows:

$$f(x) = \left( \frac{x}{|x|+1} \right) \quad (29)$$

Where the absolute input value is denoted as  $|x|$ . The major variation in tanh and Softsign functions is the rate of convergence, wherein tanh, is in the exponential form and Softsign, is in the form of a polynomial.

## 4. Results and discussion

The performance of the proposed technique is simulated through Python environment with system

requirements: RAM of 16GB, Intel core i7 processor, and Windows 10 (64 bit) operating system. The performance of the proposed ASA-LSTM technique is estimated in terms of segmentation and classification by the actual features, as well as after selecting the features. The performance of the ASA segmentation technique is compared with other previous techniques namely, denoising auto-encoder (DAE), sparse auto-encoder (SAE), and variational auto-encoder (VAE). The performance of ASA-LSTM classification method is compared to previous techniques namely, CNN, artificial neural network (ANN) and recurrent neural network (RNN). The outcomes of the segmentation and classification are discussed in the below subsections.

### 4.1 Evaluation for segmentation

The segmentation process using ASA is evaluated based on the performance measures, DSC, and HD for various tumor regions of TC, ET, and WT. *Table 1* represents the performance of the segmentation process for various regions. The proposed ASA method for the segmentation process attains DSC of 96.59%, 96.18% and 95.94%, and HD of 12.16, 12.68, and 13.05 for TC, ET and WT tumor regions respectively, which are clearly superior values than those of previous techniques.

**Table 1** Performance evaluation of segmentation process

Methods	DSC (%)			HD (mm)		
	TC	ET	WT	TC	ET	WT
DAE	91.48	89.28	90.73	20.58	19.83	19.87
SAE	93.27	91.79	92.00	18.25	17.94	18.04
VAE	94.06	93.68	93.16	13.73	15.85	16.48
ASA	96.59	96.18	95.94	12.16	12.68	13.05

### 4.2 Evaluation for classification

The classification process using ASA-LSTM with default features is analyzed based on the performance metrics of accuracy, precision, recall, and F1-Score for various tumor regions. *Table 2* represents the performance of the classification process with default features. The proposed ASA-LSTM method for the classification process attains the accuracies of 99.40%, 99.35% and 99.27% for TC, ET and WT tumor regions respectively, which is more effective than the existing techniques.

The classification process using ASA-LSTM after feature selection is analyzed for various tumor regions. After the feature extraction, the relevant features are selected by using WOA which minimizes the irrelevant features and maximizes the classification performance. *Table 3* demonstrates the outcomes of the classification process after feature selection. The proposed ASA-LSTM method for the classification process attains the accuracies of 99.48%, 99.44% and 99.32% for TC, ET and WT tumor regions respectively, which surpasses the existing methods.

**Table 2** Performance evaluation of classification with default features

Methods	Accuracy (%)			Precision (%)			Recall (%)			F1-Score (%)		
	TC	ET	WT	TC	ET	WT	TC	ET	WT	TC	ET	WT
CNN	95.20	94.56	94.76	95.97	96.04	94.25	95.18	94.49	95.38	94.79	95.69	94.62

Methods	Accuracy (%)			Precision (%)			Recall (%)			F1-Score (%)		
	TC	ET	WT	TC	ET	WT	TC	ET	WT	TC	ET	WT
ANN	97.28	97.22	97.13	96.82	97.81	95.74	96.36	95.32	96.27	95.24	96.21	95.19
RNN	98.33	98.29	98.20	96.91	96.89	97.80	96.43	97.38	97.32	97.30	97.27	97.25
ASA-LSTM	99.40	99.35	99.27	99.05	99.01	98.97	98.51	98.49	98.44	98.45	98.38	98.32

**Table 3** Performance evaluation of classification afterward feature selection

Methods	Accuracy (%)			Precision (%)			Recall (%)			F1-Score (%)		
	TC	ET	WT	TC	ET	WT	TC	ET	WT	TC	ET	WT
CNN	95.31	94.64	95.02	96.13	96.27	94.33	95.30	94.62	95.52	94.93	95.81	94.81
ANN	97.47	97.38	97.32	97.01	97.92	96.00	96.42	95.44	96.40	95.41	96.38	95.39
RNN	98.70	98.58	97.49	98.61	97.76	97.04	97.48	98.03	97.85	97.93	97.37	97.32
ASA-LSTM	99.48	99.44	99.32	99.20	99.15	99.08	98.62	98.58	98.53	98.55	98.49	98.41

From *Table 4*, it is evident that the ASA-LSTM technique consumes lesser processing time of 1.2 sec for TC, 1.7 sec for ET and 2.1 sec for WT. The memory usage of proposed method is 8 GB. The power consumption of proposed method is 27 W.

**Table 4** Performance evaluation of ASA-LSTM with processing time

Methods	Processing Time (Sec)		
	TC	ET	WT
CNN	3.9	4.4	4.8
ANN	3.3	3.8	3.9
RNN	2.2	2.7	3.2
ASA-LSTM	1.2	1.7	2.1

**Table 5** Analysis of statistical test

Tumor Region	T-Test	P-Test
TC	2.805	0.022
ET	2.681	0.025
WT	2.640	0.027

**Table 6** Comparative analysis on BraTS2020 dataset

Author	Methods	Dataset	Accuracy (%)	Precision (%)
Rao and Karunakara [38]	KSVM-SSD	BraTS 2020	99.15	99.00
Ilhan et al. [40]	Tumor localization + U-net		99.40	92.94
Proposed Method	ASA-LSTM		99.48	99.20

#### 4.4 Discussion

This research proposes an ASA-LSTM method for BraTS and classification. Min-max normalization and median filter are used in this experiment for data pre-processing which normalizes the data and minimizes the noise. The ASA method is used for image segmentation, to segment the relevant part for classification. Then, DenseNet-201 method is implemented for extracting relevant features from segmented images. Next, a WOA algorithm is used for effective selection of features, that selects relevant features for selection. This work proposes an ASA-based segmentation and a LSTM model for effective classification. The KSVM-SSD [21] and Tumor

localization+U-net [23] methods have limitations such as not being suitable for detecting a tumor in its early stages, the low-grade and high-grade tumors not being classified, negligence while extracting objects of interest, not being applicable for real time data fusion and cascading, and not identifying the substructure of tumor regions. The outcomes of the proposed ASA-LSTM technique are estimated through utilizing different tumor regions like TC, ET, and WT. The proposed method performed well while comparing to other methods, KSVM-SSD [21] and Tumor localization+U-net [23]. The proposed technique accomplishes an accuracy of 99.48%, 99.44% and 99.32% correspondingly for TC, ET, and WT tumor

#### 4.3 Comparative analysis

In *Table 5*, the statistical p-test and t-test are analyzed for various tumor regions. The statistical test is analyzed based on classification accuracy after feature selection. The TC region gains 2.805 in t-test and 0.022 in p-test. The ET region gains 2.681 in t-test and 0.025 in p-test. The WT region gains 2.640 in t-test and 0.027 in p-test.

In this section, a comparative analysis of the proposed methodology is described in *Table 6*. The performance of proposed ASA-LSTM is compared to other existing methods like KSVM-SSD [21] and Tumor localization + U-net [23] in terms of accuracy and precision. The proposed method attains accuracy of 99.48%, which surpasses the other existing techniques, KSVM-SSD which attains accuracy of 99.15% and Tumor localization + U-net that attains accuracy of 99.40%. A complete list of abbreviations is listed in *Appendix I*.

regions. This helps physicians to check the existence of abnormalities in MRIs with respect to various regions of brain. The proposed ASA-based LSTM method is much more robust to noise and effects of shading, and is mainly advantageous for locating tumor and affected parts with less objective function.

### Limitation

There is still the qualitative limitation that should be enhanced through applying much complex and deeper network architecture. The proposed method missed some label parts, while tumor segmentation.

### 5. Conclusion and future work

Early detection of brain tumors is essential for the appropriate treatment of cancer patients, which can maximize their survival rates. The BraTS – 2020 dataset is utilized in this research for segmentation and classification. A min-max normalization and median filter are used in this experiment for data pre-processing, and then fed to DenseNet-201 for extracting features from MRI images. Next, a WOA algorithm is used for effective selection of features. An ASA-based segmentation and an LSTM model for effective classification were proposed. Performance of proposed ASA-LSTM technique is estimated through utilizing different tumor regions known as TC, ET, and WT. The proposed technique accomplishes an accuracy of 99.48%, 99.44% and 99.32% correspondingly for TC, ET, and WT tumor regions, which proves that it is more robust when compared with other existing methods, CNN, ANN, and RNN. In the future, hyperparameter tuning of the classification model will be performed to improve classification efficiency.

### Acknowledgment

None.

### Conflicts of interest

The authors have no conflicts of interest to declare.

### Data availability

The BraTS 2020 dataset used in this research is publicly available at the following link: <https://www.kaggle.com/datasets/awsaf49/brats2020-training-data>.

### Author's contribution statement

**Dhyanendra Jain:** Conceptualization, investigation, data collection, interpretation of result, writing – original draft. **Amit Kumar Pandey:** Conceptualization, investigation, data collection, writing – original draft. **Alok Singh Chauhan:** Conceptualization, writing-review, and supervision. **Jitendra Singh Kushwah:** Conceptualization,

supervision. **Neeta Saxena:** Writing review and editing. **Rajeev Sharma:** Analysis result and editing. **Venkata Durga Prasad Sambrow:** Writing-review, and supervision.

### References

- [1] Vankdothu R, Hameed MA. Brain tumor segmentation of MR images using SVM and fuzzy classifier in machine learning. *Measurement: Sensors*. 2022; 24:100440.
- [2] Agrawal P, Katal N, Hooda N. Segmentation and classification of brain tumor using 3D-UNet deep neural networks. *International Journal of Cognitive Computing in Engineering*. 2022; 3:199-210.
- [3] Dang K, Vo T, Ngo L, Ha H. A deep learning framework integrating MRI image preprocessing methods for brain tumor segmentation and classification. *IBRO Neuroscience Reports*. 2022; 13:523-32.
- [4] Ahuja S, Panigrahi BK, Gandhi TK. Enhanced performance of dark-nets for brain tumor classification and segmentation using colormap-based superpixel techniques. *Machine Learning with Applications*. 2022; 7:100212.
- [5] Haq EU, Jianjun H, Huarong X, Li K, Weng L. A hybrid approach based on deep CNN and machine learning classifiers for the tumor segmentation and classification in brain MRI. *Computational and Mathematical Methods in Medicine*. 2022; 2022:1-19.
- [6] Anand L, Rane KP, Bewoor LA, Bangare JL, Surve J, Raghunath MP, et al. Development of machine learning and medical enabled multimodal for segmentation and classification of brain tumor using MRI images. *Computational intelligence and neuroscience*. 2022; 2022:1-8.
- [7] Hossain A, Islam MT, Rahman T, Chowdhury ME, Tahir A, Kiranyaz S, et al. Brain tumor segmentation and classification from sensor-based portable microwave brain imaging system using lightweight deep learning models. *Biosensors*. 2023; 13(3):1-29.
- [8] Mandle AK, Sahu SP, Gupta G. Brain tumor segmentation and classification in MRI using clustering and kernel-based SVM. *Biomedical and Pharmacology Journal*. 2022; 15(2):699-716.
- [9] Almufareh MF, Imran M, Khan A, Humayun M, Asim M. Automated brain tumor segmentation and classification in MRI using YOLO-based deep learning. *IEEE Access*. 2024; 16189-207.
- [10] Jiang Y, Zhang Y, Lin X, Dong J, Cheng T, Liang J. SwinBTS: a method for 3D multimodal brain tumor segmentation using swin transformer. *Brain Sciences*. 2022; 12(6):1-15.
- [11] Atia N, Benzaoui A, Jacques S, Hamiane M, Kourd KE, Bouakaz A, et al. Particle swarm optimization and two-way fixed-effects analysis of variance for efficient brain tumor segmentation. *Cancers*. 2022; 14(18):1-32.
- [12] Mostafa AM, Zakariah M, Aldakheel EA. Brain tumor segmentation using deep learning on MRI images. *Diagnostics*. 2023; 13(9):1-22.
- [13] Raza A, Ayub H, Khan JA, Ahmad I, S SA, Daradkeh YI, et al. A hybrid deep learning-based approach for

- brain tumor classification. *Electronics*. 2022; 11(7):1-22.
- [14] Shiny KV. Brain tumor segmentation and classification using optimized U-Net. *The Imaging Science Journal*. 2024; 72(2):204-19.
- [15] Samee NA, Ahmad T, Mahmoud NF, Atteia G, Abdallah HA, Rizwan A. Clinical decision support framework for segmentation and classification of brain tumor MRIs using a U-Net and DCNN cascaded learning algorithm. *Healthcare*. 2022; 10:1-23.
- [16] Li X, Bellotti R, Meier G, Bachtiry B, Weber D, Lomax A, et al. Uncertainty-aware MR-based CT synthesis for robust proton therapy planning of brain tumour. *Radiotherapy and Oncology*. 2024; 191:110056.
- [17] Sarabi MS, Ma SJ, Jann K, Ringman JM, Wang DJ, Shi Y. Vessel density mapping of small cerebral vessels on 3D high resolution black blood MRI. *Neuroimage*. 2024; 286:120504.
- [18] Ansari AS. Numerical simulation and development of brain tumor segmentation and classification of brain tumor using improved support vector machine. *International Journal of Intelligent Systems and Applications in Engineering*. 2023; 11(2s):35-44.
- [19] Aleid A, Alhussaini K, Alanazi R, Altwaimi M, Altwijri O, Saad AS. Artificial intelligence approach for early detection of brain tumors using MRI images. *Applied Sciences*. 2023; 13(6):1-11.
- [20] Jabbar A, Naseem S, Mahmood T, Saba T, Alamri FS, Rehman A. Brain tumor detection and multi-grade segmentation through hybrid caps-VGGNet model. *IEEE Access*. 2023; 11:72518-36.
- [21] Ahmadi M, Sharifi A, Jafarian FM, Soleimani N. Detection of brain lesion location in MRI images using convolutional neural network and robust PCA. *International Journal of Neuroscience*. 2023; 133(1):55-66.
- [22] Reddy KR, Dhuli R. A novel lightweight CNN architecture for the diagnosis of brain tumors using MR images. *Diagnostics*. 2023; 13(2):1-11.
- [23] Athisayamani S, Antonyswamy RS, Sarveshwaran V, Almeshari M, Alzamil Y, Ravi V. Feature extraction using a residual deep convolutional neural network (ResNet-152) and optimized feature dimension reduction for MRI brain tumor classification. *Diagnostics*. 2023; 13(4):1-20.
- [24] Özkaya Ç, Sağiroğlu Ş. Glioma grade classification using CNNs and segmentation with an adaptive approach using histogram features in brain MRIs. *IEEE Access*. 2023; 11:52275-87.
- [25] Kurdi SZ, Ali MH, Jaber MM, Saba T, Rehman A, Damaševičius R. Brain tumor classification using meta-heuristic optimized convolutional neural networks. *Journal of Personalized Medicine*. 2023; 13(2):1-18.
- [26] Saladi S, Karuna Y, Koppu S, Reddy GR, Mohan S, Mallik S, et al. Segmentation and analysis emphasizing neonatal MRI brain images using machine learning techniques. *Mathematics*. 2023; 11(2):1-20.
- [27] Sille R, Choudhury T, Sharma A, Chauhan P, Tomar R, Sharma D. A novel generative adversarial network-based approach for automated brain tumour segmentation. *Medicina*. 2023; 59(1):1-17.
- [28] Akter A, Nosheen N, Ahmed S, Hossain M, Yousuf MA, Almoyad MA, et al. Robust clinical applicable CNN and U-Net based algorithm for MRI classification and segmentation for brain tumor. *Expert Systems with Applications*. 2024; 238:122347.
- [29] Nassar SE, Yasser I, Amer HM, Mohamed MA. A robust MRI-based brain tumor classification via a hybrid deep learning technique. *The Journal of Supercomputing*. 2024; 80(2):2403-27.
- [30] Abd EBS, Nasr ME, Khamis S, Ashour AS. Btc-fcnn: fast convolution neural network for multi-class brain tumor classification. *Health Information Science and Systems*. 2023; 11(1):1-22.
- [31] Pasnoori N, Flores-garcia T, Barkana BD. Histogram-based features track Alzheimer's progression in brain MRI. *Scientific Reports*. 2024; 14(1):1-12.
- [32] Nodirov J, Abdusalomov AB, Whangbo TK. Attention 3D U-net with multiple skip connections for segmentation of brain tumor images. *Sensors*. 2022; 22(17):1-17.
- [33] Walsh J, Othmani A, Jain M, Dev S. Using U-net network for efficient brain tumor segmentation in MRI images. *Healthcare Analytics*. 2022; 2:100098.
- [34] Kibriya H, Masood M, Nawaz M, Nazir T. Multiclass classification of brain tumors using a novel CNN architecture. *Multimedia Tools and Applications*. 2022; 81(21):29847-63.
- [35] Mowlani K, Jafari SM, Hashemipour M. Segmentation and classification of brain tumors using fuzzy 3D highlighting and machine learning. *Journal of Cancer Research and Clinical Oncology*. 2023; 149(11):9025-41.
- [36] Amin J, Anjum MA, Gul N, Sharif M. A secure two-qubit quantum model for segmentation and classification of brain tumor using MRI images based on blockchain. *Neural Computing and Applications*. 2022; 34(20):17315-28.
- [37] Deepa S, Janet J, Sumathi S, Ananth JP. Hybrid optimization algorithm enabled deep learning approach brain tumor segmentation and classification using MRI. *Journal of Digital Imaging*. 2023; 36(3):847-68.
- [38] Rao CS, Karunakara K. Efficient detection and classification of brain tumor using kernel based SVM for MRI. *Multimedia Tools and Applications*. 2022; 81(5):7393-417.
- [39] Nanda A, Barik RC, Bakshi S. SSO-RBNN driven brain tumor classification with saliency-K-means segmentation technique. *Biomedical Signal Processing and Control*. 2023; 81:104356.
- [40] Ilhan A, Sekeroglu B, Abiyev R. Brain tumor segmentation in MRI images using nonparametric localization and enhancement methods with U-net. *International Journal of Computer Assisted Radiology and Surgery*. 2022; 17(3):589-600.
- [41] Habib H, Amin R, Ahmed B, Hannan A. Hybrid algorithms for brain tumor segmentation, classification and feature extraction. *Journal of Ambient Intelligence and Humanized Computing*. 2022; 13(5):2763-84.

- [42] Khairandish MO, Sharma M, Jain V, Chatterjee JM, Jhanjhi NZ. A hybrid CNN-SVM threshold segmentation approach for tumor detection and classification of MRI brain images. *IRBM*. 2022; 43(4):290-9.
- [43] Budati AK, Katta RB. An automated brain tumor detection and classification from MRI images using machine learning techniques with IoT. *Environment, Development and Sustainability*. 2022; 24(9):10570-84.
- [44] Nawaz SA, Khan DM, Qadri S. Brain tumor classification based on hybrid optimized multi-features analysis using magnetic resonance imaging dataset. *Applied Artificial Intelligence*. 2022; 36(1):2031824.
- [45] Chahal PK, Pandey S. A hybrid weighted fuzzy approach for brain tumor segmentation using MR images. *Neural Computing and Applications*. 2023; 35(33):23877-91.
- [46] Rahman T, Islam MS. MRI brain tumor detection and classification using parallel deep convolutional neural networks. *Measurement: Sensors*. 2023; 26:100694.
- [47] Tseng CJ, Tang C. An optimized XGBoost technique for accurate brain tumor detection using feature selection and image segmentation. *Healthcare Analytics*. 2023; 4:100217.
- [48] Gupta V, Bibhu V. Deep residual network based brain tumor segmentation and detection with MRI using improved invasive bat algorithm. *Multimedia Tools and Applications*. 2023; 82(8):12445-67.
- [49] Saurav S, Sharma A, Saini R, Singh S. An attention-guided convolutional neural network for automated classification of brain tumor from MRI. *Neural Computing and Applications*. 2023; 35(3):2541-60.
- [50] <https://www.kaggle.com/datasets/awsaf49/brats2020-training-data>. Accessed 24 March 2024.
- [51] Kordnoori S, Sabeti M, Shakoor MH, Moradi E. Deep multi-task learning structure for segmentation and classification of supratentorial brain tumors in MR images. *Interdisciplinary Neurosurgery*. 2024; 36:101931.
- [52] Minarno AE, Kantomo IS, Sumadi FD, Nugroho HA, Ibrahim Z. Classification of brain tumors on MRI images using densenet and support vector machine. *JOIV: International Journal on Informatics Visualization*. 2022; 6(2):404-10.
- [53] Riyahi M, Rafsanjani MK, Gupta BB, Alhalabi W. Multiobjective whale optimization algorithm-based feature selection for intelligent systems. *International Journal of Intelligent Systems*. 2022; 37(11):9037-54.



**Dr. Dhyanendra Jain** is currently working as an Assistant Professor (Sr. Scale) in Department of CSE-AIML, ABES Engineering College, Ghaziabad affiliated to AKTU, U.P., India. He previously worked with Dr. Akhilesh Das Gupta Institute of Technology and Management New Delhi, ITM College, Gwalior, gaining more than Eleven years of rich experience in research working in academia. He has attended national

and international conferences as a session chair and been a keynote speaker in various platforms. He was awarded best teacher, best researcher, and extra academic performer. He has published patents, books and research papers in various national and international conferences and journals. His research area includes Artificial Intelligence, Machine Learning and Data Mining.

Email: dhyanendra.jain@gmail.com



**Amit Kumar Pandey** is currently providing service as an Assistant Professor (Sr. Scale) at Department of CSE-DS, ABES Engineering College, Ghaziabad affiliated to AKTU, U.P., India. He previously worked with many renowned Engineering Institute gaining more than Eleven years of rich experience in research and academic. There are no.'s of conferences and seminars he attended as keynote speaker. He is also an active member of different Technical bodies working in computer science field. He has published patents, books and research papers in various national and international conferences and journals. His research area includes Artificial intelligence, Machine Learning and Information Security.

Email: amitpandey33@gmail.com



**Dr. Alok Singh Chauhan** is currently working as an Associate Professor in the School of Computer Applications and Technology, Galgotias University, Greater Noida, India. He is a researcher, academician and technologist, who wants to do innovative research, share and impart knowledge in the area of Data Mining, Big Data, Machine Learning and Deep Learning. He has done MCA, M.Tech (Information Technology), Executive PGDM (Information Systems Management), and Ph.D. He received a Ph.D. degree in Computer Application from Bundelkhand University, Jhansi, India. He has over 17 years of rich experience in academia and research. He is a member of the International Association of Engineers (IAENG), IEEE and ACM. He was honored as session chair & reviewer in various international conferences and served as resource person in FDPs. He has published numerous research papers in national and international journals and conferences. He has received outstanding paper as well as best paper awards. He has numerous patents and book chapters also to his credit.

Email: alok.chauhan@galgotiasuniversity.edu.in



**Dr. Jitendra Singh Kushwah** completed his Ph.D. in Computer Science & Engineering from Rabindranath Tagore University, Bhopal, MP. He has extensive experience in teaching and research in Machine Learning, Data Mining, and Data Science. Dr. Kushwah has published numerous articles in journals and conferences, and

has authored books and book chapters. He holds patents and copyrights. Currently, he serves as an Associate Professor in Computer Science & Engineering at the Institute of Technology and Management in Gwalior, MP, India. He has chaired various sessions and served as a resource person, delivering expert lectures at different institutions and universities. He has received multiple academic awards.

Email: Jitendra.singhkushwah@itmgoi.in



**Dr. Neeta Saxena** completed her Ph.D. in Mathematics from Jiwaji University, Gwalior, MP. She has taught and conducted research in the area of Applied Mathematics for the last 10 years. Dr. Saxena has published 18 research papers in applied mathematics and has over 25 years of teaching experience in reputed institutes across Madhya Pradesh. Currently, she is working as an Associate Professor at SAGE University, Bhopal, MP.

Email: neetasaxenagwl@gmail.com



**Dr. Rajeev Sharma** completed his Ph.D. in Computer Science & Engineering from Rabindranath Tagore University, Bhopal, MP. He has taught and conducted research in the areas of Data Mining and Data Science. He has published many articles in journals and conferences and written books and book chapters. He has patents and copyrights to his credit. Currently, he is working as an Assistant Professor in Computer Science at Government College Kailaras, Morena, MP, India. He has chaired many sessions and served as a resource person, delivering expert lectures at various institutes and universities.

Email: sharmaraj2007@gmail.com



**Venkata Durga Prasad Sambrow** is currently working as an Assistant Professor in the Department of Computer Science & Engineering with Data Science, Chalapathi Institute of Engineering & Technology, Lam, Guntur, A.P., India affiliated to Acharya Nagarjuna University. He is a researcher, academican and technologist, who wants to do innovative research, share and impart knowledge in the area of Net work security, Data Science, Machine Learning and Deep Learning. He has done MCA, M.Tech., (Computer Science Engineering), B.Ed., (Maths), and pursuing Ph.D. He has 18 years of experience in academia and research. He is a member of the Research Foundation of India. He was attended many international conferences, Seminars, Workshops, International / National FDP's . He has published more than 4 research papers in National/International Journals of repute.

Email: prasadsvd999@gmail.com

## Appendix I

S. No.	Abbreviation	Description
1	ASA	Attentive Symmetric Auto-Encoder
2	AG-CNN	Attention-Guided Convolutional Neural Network
3	ANN	Artificial Neural Network
4	BA	Bat Algorithm
5	BraTS	Brain Tumor Segmentation
6	CJHBA	Chronological Jaya Honey Badger Algorithm
7	C-V	Chan-Vese
8	CNN	Convolutional Neural Network
9	CT	Computed Tomography
10	CLAHE	Contrast-Limited Adaptive Histogram Equalization
11	COM	Co-occurrence Matrix
12	DAE	Denosing Auto-Encoder
13	DL	Deep Learning
14	DNN	Deep Neural Network
15	DCNN	Deep Convolutional Neural Network
16	DRN	Deep Residual Network
17	DSC	Dice Score Coefficient
18	EEG	Electroencephalogram
19	ET	Enhancing Tumor
20	GA-DNN	Genetic Algorithm Deep Neural Network
21	GOA-SVM	Grasshopper Optimization Algorithm – Support Vector Machine
22	GLCM	Gray Level Co-Occurrence Matrix
23	SGLCM	Spatial Gray Level Co-Occurrence Matrix
24	HBA	Honey Badger Algorithms
25	HHO	Harris Hawks Optimization
26	HBTC	Hybrid-Brain-Tumor-Classification
27	HD	Hausdorff Distance
28	IIB	Improved Invasive Bat
29	IDM	Inverse Difference Moment
30	IWO	Invasive Weed Optimization
31	KNN	K-Nearest Neighbor
32	KSVM-SSD	Kernal Support Vector Machine-Social Ski Driver
33	SegCNN	Segment Convolutional Neural Network
34	LSTM	Long Short-Term Memory
35	MLT	Machine Learning Technique
36	MRI	Magnetic Resonance Images
37	MSE	Mean Squared Error
38	PDCNN	Parallel Deep Convolutional Neural Network
39	PSO	Particle Swarm Optimization
40	RBNN	Radial Basis Neural Network
41	RNN	Recurrent Neural Network
42	RLM	Run-Length Matrix
43	SPE	Symmetric Position Encoding
44	SHA	Secure Hash Algorithm
45	SSO	Social Spider Optimization
46	STM	Software Transactional Memory
47	SAE	Sparse Auto-Encoder
48	SVM	Support Vector Machine
49	SSD	Social Ski Driver
50	TC	Tumor Core
51	VAE	Variational Auto-Encoder
52	WFKM	Weighted Fuzzy K-Means
53	WOA	Whale Optimization Algorithm
54	WT	Whole Tumor
55	XGBoost	Extreme Gradient Boosting
56	2D-FLAIR	2Dimensional Fluid-Attenuated Inversion Recovery
57	3DVHOG	3D Voxel based extension of the 2D Histogram of Oriented Gradients